J. Fluid Mech. (1989), *vol.* 209, *pp.* 501–519
Printed in Great Britain

The influence of pressure-dependent density and viscosity on the elastohydrodynamic collision and rebound of two spheres

By GUY BARNOCKY AND ROBERT H. DAVIS
Department of Chemical Engineering, University of Colorado, Boulder, CO 80309-0424, USA

(Received 1 September 1988 and in revised form 7 June 1989)

A theoretical description of the low-Reynolds-number collision and rebound of two rigid or elastic spheres separated by a thin layer of viscous fluid with pressure-dependent physical properties is presented. It has previously been shown by Davis *et al.* (1986) that the hydrodynamic pressure which builds up in the thin fluid layer must become large enough to elastically deform the spheres near the axis of symmetry, if they are to rebound subsequent to colliding. Under these extreme pressures, however, it is expected that the fluid may also compress and that its viscosity may increase by several orders of magnitude. It is shown that these pressure-dependent effects may significantly alter the minimum separation reached during approach of the spheres, as well as the maximum separation and relative velocity attained during rebound of the spheres. In particular, the pressure buildup during the collision process is predicted to become sufficiently large under some conditions so that the corresponding viscosity increase causes the fluid in the gap between the colliding spheres to behave nearly as a solid and to limit the close approach of the opposing surfaces. Also, the storage of energy via the compression of the fluid in the gap allows rigid spheres to bounce as this energy is released subsequent to their collision. However, it is found that this rebound is very weak relative to that which is predicted for elastic spheres.

1. Introduction

Energetic collisions between solid bodies in fluids are an integral part of many industrial and natural processes such as filtration, lubrication and erosion. In modelling the fundamental mechanisms which underlie these systems, it is necessary to establish criteria for whether the solid bodies will adhere or bounce apart after colliding. The original theory of Hertz and its extensions (see Love 1927; Dahneke 1971; Loffler 1980) neglect the influence of the surrounding fluid, and predict that colliding spheres will adhere upon impact unless the incoming kinetic energy exceeds a critical value, based on an interparticle adhesive force and energy losses in the contacting solids. However, several workers (Tabor 1949; Butler 1960; Christensen 1962; Finkin 1973) have observed experimentally that the presence of a lubricant may have a significant influence on the dynamics of colliding elastic bodies. Surprisingly, for impacts leaving a dent due to plastic deformation of the surfaces in these experiments, the deformations were found to be deeper in the presence of a lubricant than without. In order to explain this finding, Christensen (1970) developed the appropriate equations and presented an approximate numerical solution (valid only for relatively large separations) to the problem of elastic

deformation of two spheres in normal approach in an incompressible fluid. Assuming an exponential dependence of the viscosity on the hydrodynamic pressure, he showed that the changes in pressure due to viscosity are concentrated in a small region near the axis of symmetry and dominate those resulting from elastic deformation until the separation between the approaching spheres becomes very small. Further, he found that the transition film thickness at which this change takes place is sharply defined and quite small, even compared to the surface roughness. These results were supported by Herrebrugh (1970) and Lee & Cheng (1973) who studied two lubricated cylinders moving toward one another under a constant force. Unfortunately, these elastohydrodynamic lubrication studies focused only on the approach portion of the collision and did not consider the possibility of rebound.

Davis, Serayssol & Hinch (1986) were the first to consider both the deformation and rebound processes for two inertially driven, elastic spheres of arbitrary radii in near-contact, head-on motion in a viscous fluid under conditions of low Reynolds number. They showed that the large pressure that develops as the fluid is being squeezed outward from the gap has several effects. First, unless the inertia of the particles is very high, it opposes their relative motion and slows their approach. Second, it may cause the surfaces to deform in a small region around the axis of symmetry. When the latter occurs, a portion of the incoming kinetic energy of the particles becomes stored as elastic strain energy of deformation, and a portion is dissipated by viscous forces. If the elastic deformation is significant, the spheres may rebound after coming to rest, although the distance of rebound is limited because further viscous dissipation occurs as the surfaces recede and fluid flows back into the gap under suction.

The magnitude of the pressure that develops during the collision, which may become as high as several hundred atmospheres or more at the axis of symmetry (see Tabor 1949), suggests that a significant increase in the density and viscosity of the fluid in the gap may occur. An increase in the fluid viscosity may alter the collision dynamics by increasing the hydrodynamic pressure and viscous dissipation, though it cannot by itself store energy which can later be released for rebound. On the other hand, an increased fluid density may result in rebound of even perfectly rigid spheres, if enough of the kinetic energy of the spheres becomes stored in the compressed fluid, and then released during the subsequent expansion of the fluid. Motivated by these considerations, the study described in this paper makes quantitative predictions of the influences of the pressure-dependent fluid properties of density and viscosity on the collision between both rigid and elastic spheres in a viscous fluid.

2. Theoretical development

Figure 1 shows the area of contact of two elastic spheres as they approach each other along their line-of-centres. In the limit as the radius of one sphere goes to infinity, the problem becomes that of a sphere impacting a plane. We seek to describe the dynamic shape of the smooth, deformable particle surfaces and the hydrodynamic force resisting their relative motion as functions of radial position, gap thickness and properties of the particles and of the surrounding fluid. The complete mathematical development of the governing equations with constant fluid properties has been previously described (Davis *et al.* 1986) and is extended here to include the pressure dependence of the fluid density and viscosity.

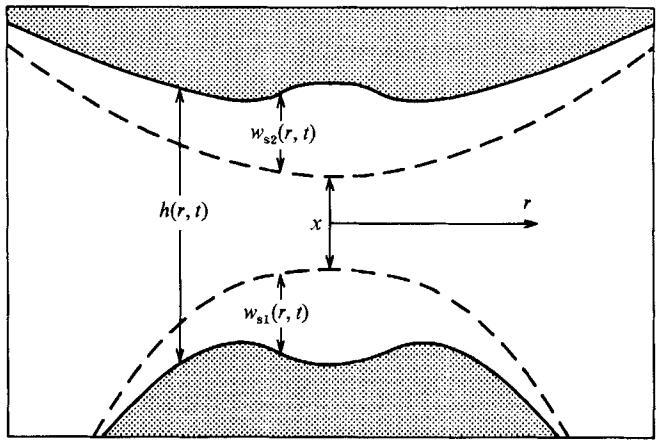

FIGURE 1. Schematic of the deformed surfaces of two colliding spheres in a viscous fluid. The dashed lines represent the undeformed surfaces.

The undeformed spherical surfaces can be approximated by paraboloids in the region of near contact, and the deformed gap profile is therefore given by

$$h(r,t) = x(t) + \frac{r^2}{2a} + w_s(r,t), \tag{1}$$

where r denotes the radial distance from the centreline, $x(t)$ is the distance between the undeformed surfaces at the centreline as a function of time, and $w_s(r,t) = w_{s1} + w_{s2}$ is the sum of the dynamic deformations of the solid surfaces from their original shape, where the subscript s denotes solid deformation and the subscripts 1 and 2 refer to the two surfaces.

As the spheres approach, a normal surface stress, $f(r,t)$, may arise from the hydrodynamic pressure in the fluid being squeezed out between their solid surfaces and from a disjoining pressure resulting from interparticle van der Waals attractive forces and electrostatic repulsive forces. This surface stress may slightly deform the solids, and, assuming that linear elasticity theory applies, the magnitude of the solid deformation, w_s, can be determined by integrating the surface stress distribution multiplied by a Green's function, $\phi(r,y)$, over the area subjected to the stress:

$$w_s(r,t) = 4\theta \int_0^\infty f(y,t)\,\phi(r,y)\,\mathrm{d}y. \tag{2}$$

The parameter θ, which contains the material properties of the elastic solids, and the kernel $\phi(r,y)$ have been defined by Davis *et al.* (1986).

The effects of a disjoining pressure arising from interparticle van der Waals attractive forces and electrostatic repulsive forces during the collision process have been recently evaluated by Serayssol & Davis (1986). In general, they found for particles with sufficient inertia to deform significantly that the hydrodynamic pressure dominates the disjoining pressure during the collision, though the attractive van der Waals forces may become significant during the last stages of approach when the surfaces are very close together. Consequently, in the present analysis, the surface stress is dominated by the hydrodynamic pressure ($f \approx p$), and the attractive van der Waals forces are assumed to be negligible.

The deformed shape of the particle surfaces cannot be determined without knowledge of the pressure profile in the fluid layer between the solid surfaces. Since we are primarily interested in the case where the surfaces are very close to one another, the fluid flow within the narrow gap between them is fully developed to leading order, and can be described by the lubrication equation of fluid dynamics which relates the rate of change of the gap size to the pressure:

$$\frac{\partial(\rho h)}{\partial t} = \frac{1}{12r}\frac{\partial}{\partial r}\left(\frac{\rho r h^3}{\mu}\frac{\partial p}{\partial r}\right), \tag{3}$$

where $p(r,t)$ is the pressure profile in the fluid layer, $\mu(p)$ is the fluid viscosity, and $\rho(p)$ is the fluid density. Note that the fluid inertia terms were assumed to be small in the derivation of (3). As discussed previously by Davis *et al.* (1986), this is valid provided that $Re\, x/a \ll 1$, where the instantaneous Reynolds number is defined by $Re = \rho v a/\mu$, and v is the relative velocity of the two spheres.

In order to solve (1)–(3) for the dynamic separation and hydrodynamic pressure, the functional dependence of density and viscosity on the pressure must be known. Studies by Grubin & Vinogradova (1949) show that the limit of the compression of viscous liquids such as mineral oil is about 25%, giving a maximum density increase of about 33%. An expression that closely fits the experimental data for mineral oil (ASME 1953), and can be used to describe the behaviour of many viscous liquids, is of the form (Dowson & Higginson 1977)

$$\frac{\rho}{\rho_0} = 1 + \frac{\hat{\alpha} p}{1 + 3\hat{\alpha}|p|}, \tag{4}$$

where ρ_0 is the density of the fluid under ambient pressure, and $\hat{\alpha}$ is a compressibility parameter which is tabulated (see Weast 1974) for various liquids and is typically on the order of 10^{-4} atm^{-1}. The absolute value of the pressure in the denominator of (4) constrains the liquid density above a value of $2\rho_0/3$ for the rebound portion of the collision, during which the surfaces recede and the pressure drops below zero. In practice, however, the density will not reach this value because cavitation will occur when the tensile pressure during rebound drops below the vapour pressure of the liquid. Thus, (4) does not apply for large negative pressures.

Until recently, the most common method of describing the variation of viscosity with pressure was by means of an exponential relation, $\mu = \mu_0 \exp(Cp)$, where μ_0 is the viscosity of the fluid under ambient pressure and C is a coefficient dependent on the fluid type (Hersey & Hopkins 1954). This relation has been extensively used in theoretical lubrication studies but it overestimates the viscosity by several orders of magnitude at high pressures (Chu & Cameron 1962). In order to alleviate this inaccuracy, a power-law relationship, which more closely approximates experimental data, has been proposed (Chu & Cameron 1962):

$$\mu = \mu_0(1 + \hat{\eta} p)^{16}, \tag{5}$$

where the viscosity coefficient $\hat{\eta}$ is a tabulated function of temperature for various liquids and is typically on the order of 10^{-4} atm^{-1}. Because of its improved accuracy at high pressures, the power-law expression has been chosen over the exponential relation in the present analysis, although the results are qualitatively independent of which viscosity–pressure relationship is chosen. If during rebound the magnitude of the tensile pressure approaches $\hat{\eta}^{-1}$, then the viscosity is predicted by (5) to approach zero. Clearly, therefore, this equation does not apply at very large negative pressures.

Note that we only consider liquids in this analysis of density and viscosity effects. Scaling arguments show that before any significant change can occur in these properties during collisions between aerosols, the separation between the surfaces drops below the mean free path of the gas molecules, the rarefied gas remaining in the gap slips out, and the spheres make physical contact (Hocking 1973; Barnocky & Davis 1988*a*). Moreover, (4) and (5) provide direct relationships between the instantaneous fluid properties and the instantaneous pressure. This implies that the fluid equilibrates rapidly with respect to the timescale of the pressure changes.

To complete the formulation of the basic model, we also need the kinematic equations, which describe the relative motion of the undeformed surfaces of the solid spheres:

$$m\frac{\mathrm{d}v}{\mathrm{d}t} = -F(t), \tag{6}$$

$$\frac{\mathrm{d}x}{\mathrm{d}t} = -v(t), \tag{7}$$

where $v(t)$ is the dimensionless relative velocity of the centre of masses of the two spheres toward one another, m is the reduced mass of the two spheres, and

$$F(t) = 2\pi \int_0^\infty f(r,t)\, r\, \mathrm{d}r$$

is the total normal force exerted between the spheres. It is assumed in (6) that the motion of the particles during the final stages of collision is due to their inertia and that the effects of any bulk flow or external force such as gravity are negligible.

Davis *et al.* (1986) solved (1)–(3), (6) and (7) under conditions of constant fluid properties, using asymptotic techniques in the limit of small deformation of the spheres, and numerical methods in the general case for which the deformation was comparable with the gap size. We have performed a similar analysis to investigate the influence of the pressure dependence of the fluid density and viscosity on collisions between solid spheres. Key issues that are addressed include whether or not fluid compression alone may be significant enough to cause a bounce subsequent to collision, and the degree to which the viscosity and density changes affect the overall collision and rebound process.

3. Method of solution

As demonstrated by Davis *et al.* (1986) for constant fluid properties (i.e. $\mu = \mu_0$, $\rho = \rho_0$), the pressure profile which develops between two colliding rigid spheres is

$$p(r,t) = \frac{3\mu_0 a v}{(x + r^2/2a)^2},$$

which is a function of both the relative velocity of the spheres, v, and the separation distance, x, each of which decreases with time according to the solution of (6) and (7). The hydrodynamic resistance which results from this pressure distribution is $F = 6\pi\mu_0 a^2 v/x$. To obtain a relationship between the relative velocity and the gap width, we divide (7) by (6), and then, utilizing the above expression for the hydrodynamic force, F, we may integrate the result to obtain

$$\frac{v}{v_0} = 1 - \frac{\ln(x_0/x)}{St}, \tag{8}$$

where we have used the initial conditions $v = v_0$ at $x = x_0$. In (8), the Stokes number, $St = mv_0/6\pi\mu_0 a^2$, provides a measure of the inertia of the particles relative to the viscous forces in the fluid. The Stokes number is also a measure of the relative importance of the initial particle kinetic energy to the inelastic work required to squeeze the fluid out of the gap, $St = mv_0^2/Fx_0$, where F is given by the asymptotic analysis above. This leads to a prediction that particles experience a detectable rebound when $St \geqslant 2$ and have sufficient energy to rebound past x_0 when $St \geqslant 4$.

3.1. *Order-of-magnitude analysis and scaling*

The asymptotic solution above is valid only for small fluid property changes and nearly inelastic collisions. In this section, we determine under what conditions density and viscosity changes will significantly affect the collision. From (2), Hertz contact theory of linear elasticity, the magnitude of solid deformation of a spherical particle, w_s, is $O(p\theta(ax)^{\frac{1}{2}})$ near the axis of symmetry, where p is a characteristic fluid pressure in the narrow gap. Using (4), an order-of-magnitude estimate for the change in the separation distance between the two surfaces due to liquid compression, w_1, is $O(\hat{\alpha}xp)$ near the axis of symmetry, where $w_1 \equiv h(\rho/\rho_0 - 1)$. Using the dynamic lubrication pressure scale, $p = O(\mu av/x^2)$, these estimates lead to the separation lengthscales, $x_1 = (4\theta\mu a^{\frac{3}{2}}v)^{\frac{2}{5}}$ and $x_2 = (\hat{\alpha}\mu av)^{\frac{1}{2}}$, at which solid deformation and fluid compression, respectively, become comparable with the separation distance, x. (The factor of 4 in the expression for x_1 is a matter of choice and comes directly from (2).) Similarly, viscosity effects become important at a separation of $x_3 = (\hat{\eta}\mu av)^{\frac{1}{2}}$, although an estimate of the physical change in the gap due solely to viscosity effects cannot be readily obtained from scaling arguments. Thus, if the value of the inertia parameter, St, is sufficiently large that the relative velocity is non-negligible when x becomes as small as x_2 or x_3 (see (8)), and if x_2 and/or x_3 is comparable with or larger than x_1, the density and/or viscosity changes in the fluid are expected to have a significant influence on the collision and rebound process. Estimates of these lengthscales for typical physical systems are given below.

Barnocky & Davis (1988*b*) performed an experiment in which small stainless steels balls were dropped from varying heights onto a flat plate covered with a thin layer of mineral oil. They varied the drop height until the critical height that allowed the balls to penetrate and just bounce out of the fluid layer was determined. For the conditions used in these experiments, which are similar to those that might be present in a lubricated bearing and which had physical parameters on the order of $a = 0.1$ cm, $\mu = 10$ g/cm s, $v = 100$ cm/s, $\hat{\alpha} = 10^{-10}$ cm^2/dyne, $\hat{\eta} = 10^{-11}$ cm^2/dyne, and $\theta = 10^{-13}$ cm^2/dyne, the critical separations defined above are: $x_1 \approx 0.4$ μm, $x_2 \approx 1$ μm, $x_3 \approx 0.3$ μm. For conditions that more closely approximate those present during inertial filtration of small aerosol particles when either the filter fibres or particles have been coated with a liquid to increase the capture efficiency (Gal, Tardos & Pfeffer 1985), typical physical parameters are $a = 3$ μm, $\mu = 100$ cP, $v = 50$ cm/s, $\hat{\alpha} = 10^{-10}$ cm^2/dyne, $\hat{\eta} = 10^{-10}$ cm^2/dyne, and $\theta = 10^{-12}$ cm^2/dyne, and the corresponding critical separations are all approximately equivalent: $x_1 \approx x_2 \approx x_3 \approx 0.01$ μm. Hence, in both lubrication and inertial filtration systems, fluid compression, viscosity increase effects, and solid deformation appear to become important at approximately equivalent separations. Moreover, at a separation of $x = 0.01$ μm for the typical conditions given above for inertial filtration of aerosols, the pressure in the fluid gap between the particle and collecting surfaces is on the order of 10^{10} dyne/cm^2 $\approx 10^4$ atm. (Similarly, pressures of 10^4 atm are characteristic for collisions between 0.1 cm particles at separations of 1 μm as in the experiment of

Barnocky & Davis 1988*b*.) This pressure is sufficiently high to cause significant changes in the fluid density and viscosity. Thus, this approximate analysis suggests that a more thorough investigation of the influence of fluid compression and viscosity changes on the dynamic collision process is warranted, as given in the following section.

3.2. *Numerical analysis*

The practical conditions cited in the previous section suggest that density and viscosity changes strongly affect the collision and produce or enhance rebound. Since the analysis of Davis *et al.* (1986) is valid so long as the density and viscosity are only slightly different from unity, a numerical solution to (1)–(7) must be developed. These calculations are greatly simplified by making the governing equations dimensionless. Using x_0 as a characteristic length in the axial direction, $(ax_0)^{\frac{1}{2}}$ as a characteristic length in the radial direction, and v_0 as a characteristic relative velocity, the resulting non-dimensional parameters are

$$St, \quad \alpha = \frac{\hat{\alpha}\mu_0 a v_0}{x_0^2}, \quad \eta = \frac{\hat{\eta}\mu_0 a v_0}{x_0^2}, \quad \epsilon = \frac{4\theta\mu_0 a^{\frac{3}{2}} v_0}{x_0^{\frac{5}{2}}},$$

where α and η represent measures of the density and viscosity changes relative to changes in the hydrodynamic pressure, respectively, and ϵ is a measure of solid elasticity introduced by Davis *et al.* (1986). However, a rescaling is necessary to facilitate the numerical computations since the choice of x_0 is somewhat arbitrary. For example, when only the deformation is significant, a more appropriate axial lengthscale is $x_1 = (4\theta\mu_0 a^{\frac{3}{2}} v_0)^{\frac{2}{5}}$, which, when used in place of x_0, yields a value of unity for ϵ. Similarly, when only density or viscosity changes are important, more appropriate lengthscales are $x_2 = (\hat{\alpha}\mu_0 a v_0)^{\frac{1}{2}}$ and $x_3 = (\hat{\eta}\mu_0 a v_0)^{\frac{1}{2}}$, respectively. Using the appropriate lengthscale when considering only either density, viscosity or deformation effects, the numerical routine need be executed for only a single value of the corresponding parameter α, η, or ϵ for each value of St. The solution for smaller values of these parameters may then be computed simply by matching the numerical computations with the asymptotic solution for small deformations.

We have developed a robust implicit, time-stepping algorithm to solve (1)–(7), utilizing finite-difference discretization of the time and space variables, and Newton's method to iteratively compute a solution at each point in time. The size of the time step was adjusted so that the local time-truncation error in the solution of the hydrodynamic force, $F(t)$, was kept below 1%. At each new time, the velocity and undeformed separation of the spheres were computed using (6) and (7) by forward differencing, and the pressure, density, viscosity and deformation profiles were iteratively computed from (1)–(5) starting with an initial guess based on the solution at the previous time. Equations (4) and (5) were used during rebound as well as approach, even though they are not expected to apply for very large negative pressures. The implications of this are discussed in the following section.

4. Results and discussion

In order to develop a simple estimate of the validity of our numerical results, we first utilize an approximate criterion for rebound resulting solely from the elastic deformation and restoration of two colliding spheres, as outlined by Barnocky & Davis (1988*b*). They proposed that in order for particles to rebound, they must have sufficient inertia to deform significantly. Since the separation distance at which

significant deformation of the solid surfaces occurs is x_1, they predicted that only those particles with sufficient inertia to come within a separation x_1 will bounce. Particles brought to rest by lubrication forces prior to reaching x_1 were not predicted to bounce because, under these conditions, insufficient energy becomes stored in elastic deformation prior to the spheres coming to rest. Using (8), collisions for which the particles have sufficient inertia to reach x_1 must satisfy $St > St_1^*$ where

$$St_1^* = \ln(x_0/x_1) = -\tfrac{2}{5}\ln(\epsilon). \tag{9}$$

When $St = St_1^*$, the particles have just enough energy to reach x_1 before coming to rest. For $St > St_1^*$, the particles are predicted to reach x_1 with a non-zero velocity, and the remaining energy becomes stored as elastic deformation of the solid, which, when released, causes the particles to rebound (here, rebound is defined as a reversal in the direction of the particle velocity). In order for the spheres to rebound back to their initial separation, x_0, an even higher value of St is required owing to the additional fluid dynamic resistance to relative motion as the surfaces recede from one another. However, during energetic collisions such as those that occur during the inertial filtration of liquid-coated aerosol particles (Gal *et al.* 1985), the tensile pressure required to draw fluid back into the gap as the spheres rebound can be as high as several hundred atmospheres. The fluid will easily cavitate at these high tensile stresses, and the fluid dynamic resistance to relative motion during the initial stages of rebound will be substantially less than the resistance during approach. Dowson & Taylor (1979) illustrate the complexity of the cavitation phenomenon which is beyond the scope of the current analysis and warrants further study.

Although the rebound phenomenon is complicated when including other effects which can strongly influence the collision, such as fluid density and viscosity changes, the above analysis can be extended to obtain an estimate for the corresponding critical Stokes number which gives rebound when one of these effects dominates the collision process. For example, if conditions are such that the fluid compresses significantly and the spheres are brought to rest before either elastic deformation or viscosity changes become significant enough to affect the collision, rebound will occur owing to a relaxation of the compressed fluid for all $St > St_2^*$, where

$$St_2^* = \ln(x_0/x_2) = -\tfrac{1}{2}\ln(\alpha). \tag{10}$$

Similarly, if viscosity effects are dominant, rebound will occur for all $St > St_3^*$, where

$$St_3^* = \ln(x_0/x_3) = -\tfrac{1}{2}\ln(\eta). \tag{11}$$

Note that an increase in viscosity cannot cause a bounce *per se*, since it only represents a resistance to flow rather than a storage of energy. However, when the gap between the colliding spheres becomes comparable with x_3, the viscosity of the fluid in the gap will become so large that the fluid will behave nearly as a solid. Rather than squeezing this fluid out of the gap, further approach of the spheres will result in their elastic deformation. Then, once the relative velocity of the spheres has reduced to zero, near a separation x_3, any energy stored in compression or deformation will cause the spheres to rebound. The estimates given by (9)–(11) provide good comparisons for the full numerically generated rebound predictions developed in the next two subsections.

4.1. *Numerical results for rigid spheres*

We first consider the influence of only the pressure-dependent fluid density on the dynamic collision between two rigid spheres. Of particular interest is whether or not

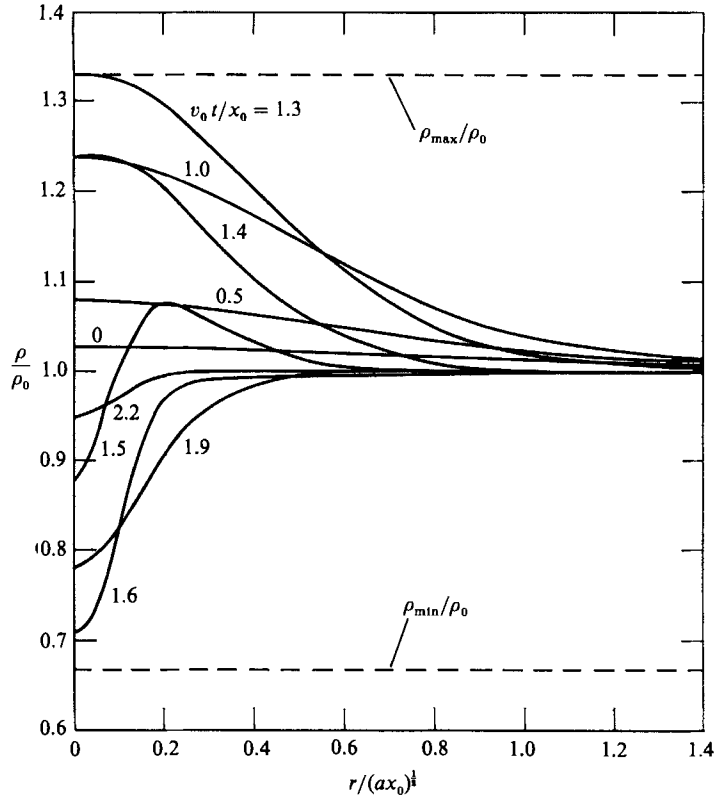

FIGURE 2. The relative fluid density profile at several instants in time for a collision between rigid spheres in an isoviscous compressible fluid with $St = 5$ and $\alpha = 10^{-2}(St_2^* = 2.3)$.

sufficient energy may become stored in the compressed fluid to allow for a significant bounce to occur. Figure 2 shows the relative density profile as a function of the dimensionless distance from the centreline for the specific case of $St = 5$, $\alpha = 10^{-2}$ at several instants in time. At $t = 0$, the fluid is only slightly compressed and the density profile can be determined using the asymptotic theory developed previously. As time progresses, and the gap between the surfaces narrows, the fluid pressure and therefore density increase. The value of the density at the centreline reaches $\rho/\rho_0 = 1.3$, which is the maximum allowed by the constitutive relation (4), at $v_0 t/x_0 \approx 1.30$. The increased fluid pressure causes the spheres to slow down, and their motion is arrested ($v = 0$) when $v_0 t/x_0 \approx 1.35$ (see figure 3). At this time, the pressure has decreased from its maximum value (but is still positive) and so the fluid is expanding. The spheres subsequently bounce owing to the expansion of the fluid. When $v_0 t/x_0$ reaches a critical value of $t_c \approx 1.49$, the density near the centreline drops below ρ_0, because a negative pressure develops which draws fluid back into the narrow gap between the receding surfaces of the rebounding spheres. This tensile stress will also cause the fluid to cavitate, assuming that its magnitude becomes greater than approximately one atmosphere. Since cavitation was not directly included in the analysis, the results for $v_0 t/x_0 > t_c$ are not expected to be accurate. Fortunately, this is not a major drawback, because the key features of arrest and rebound occur just prior to this time. As the spheres come to their final equilibrium position, both the kinetic energy of the moving spheres and the potential energy stored as fluid compression are completely dissipated in the viscous fluid.

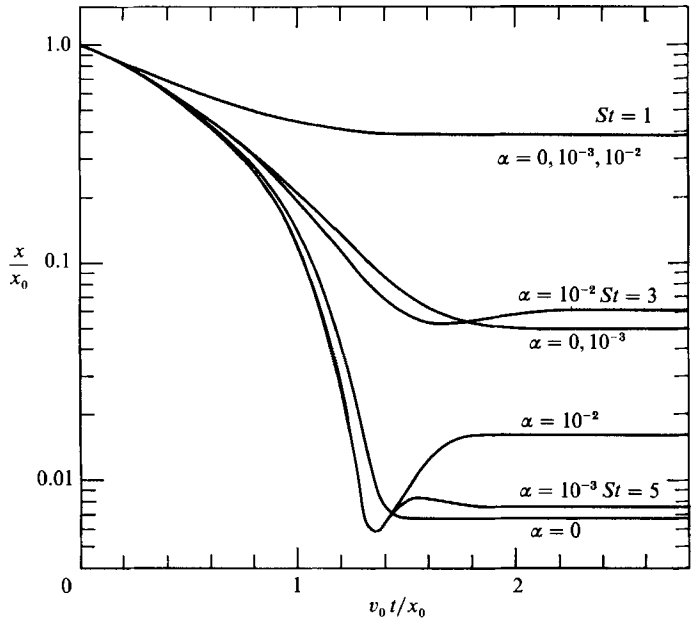

FIGURE 3. The dimensionless centreline separation as a function of the dimensionless time for collisions between rigid spheres in an isoviscous compressible fluid.

The dynamics of the collision between rigid spheres in a compressible fluid is more clearly illustrated by figure 3, a plot of the dimensionless separation at the centreline, x/x_0, as a function of dimensionless time, $v_0 t/x_0$, for $St = 1$, 3, and 5 and $\alpha = 0$, 10^{-3} and 10^{-2}. Analytical solutions for the curves in figure 3 corresponding to $\alpha = 0$ are given by (9) of Davis *et al.*(1986). For these limiting cases, the minimum distance of approach is $x/x_0 = \exp(-St)$, which is also the final separation since the fluid is incompressible and no rebound occurs. When the particle inertia or fluid compressibility is small ($St < St_2^* = -\frac{1}{2}\ln(\alpha)$), fluid compression has a negligible influence on the collision process and does not produce a rebound. On the other hand, when $St \geqslant St_2^*$, fluid compression can alter the trajectories of the approaching spheres and even cause a small bounce to occur. For $St = 3$ and $\alpha = 10^{-2}(St_2^* = 2.3)$, for example, the relative approach velocity of the spheres at a given separation is greater than for $\alpha = 0$ since the fluid can compress as well as squeeze out of the gap, thereby offering less resistance (see Barnocky 1988). Under these conditions, the spheres never reach the minimum separation predicted for a collision in an incompressible fluid ($x/x_0 = \exp(-St)$), but instead bounce at a slightly larger separation. The magnitude of the bounce is limited owing both to the relatively small solid inertia and to the fact that much of the compression energy is released prior to rebound. For $St = 5$ and $\alpha = 10^{-2}$, the spheres again have a higher relative velocity at a given separation during the initial stages of the collision, and the gap reduces to a value less than $x/x_0 = \exp(-St)$ before rebound occurs. During the later stages of rebound ($v_0 t/x_0 > t_c$), the spheres experience resistance to relative motion due to the tensile pressure in the gap between them. This brings them to rest at a final equilibrium separation. The final separation will be greater than that shown in figure 3 when cavitation occurs.

Figure 4 illustrates the dependence of the dimensionless maximum rebound

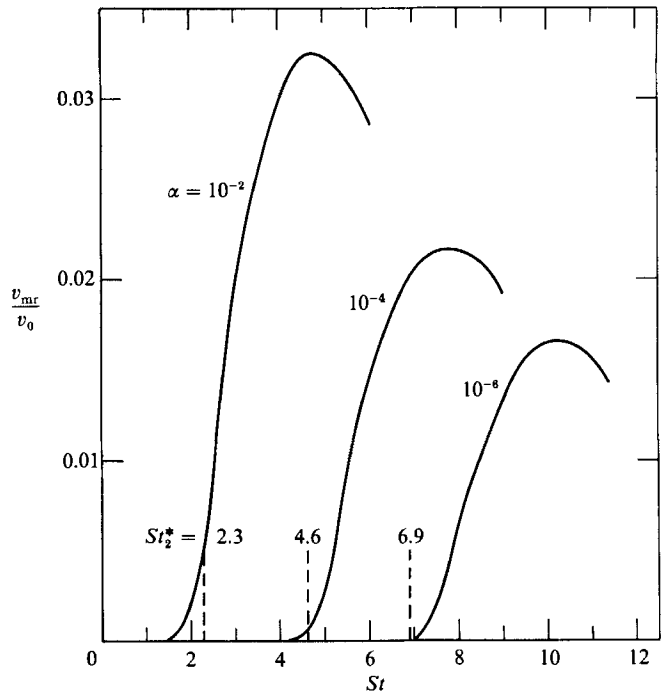

FIGURE 4. Maximum relative rebound velocity for collisions between rigid spheres in a compressible fluid as a function of the inertia parameter, St, for various values of the compressibility parameter, α.

velocity, v_{mr}/v_0, on the parameters St and α. The maximum rebound velocity, v_{mr}, is defined as the largest value of $-v$ that the spheres obtain as they rebound from one another. No rebound occurs ($v_{mr} = 0$) for all collisions for which $St \ll St_2^*(\alpha)$. For $\alpha = 10^{-2}(St_2^* = 2.3)$, a non-zero rebound velocity occurs for all $St > 1.5$. For this value of α, the dimensionless rebound velocity increases rapidly as St increases until it reaches a maximum of only 0.032 when $St = 5$. For more energetic collisions (i.e. $St \gg St_2^*$), the minimum distance of approach is less, but the fluid in the gap near the centreline cannot compress further since it is at or near its maximum density of $\rho/\rho_0 = 1.3$. Since less energy can be stored in the form of fluid compression in a narrower gap, a smaller maximum rebound velocity occurs. The other curves ($\alpha = 10^{-6}$ and 10^{-4}), which correspond to less compressible liquids and therefore relatively smaller rebound velocities, exhibit similar behaviour. Thus, although fluid compression alone can result in the rebound of two colliding rigid spheres, this rebound is generally very weak. Cavitation does not affect the maximum rebound velocity, since cavitation only occurs when the pressure of the liquid in the gap drops below its vapour pressure. By the time this occurs, the pressure in the gap is already less than the ambient pressure, and the resulting suction force is slowing down the rebounding spheres.

The final plot of this section (figure 5) illustrates the changes that may occur to the fluid viscosity during a collision between rigid spheres. This diagram shows several dimensionless viscosity profiles at different times for the specific case $St = 3.5$ and $\eta = 10^{-3}(St_3^* = 3.5)$. The fluid under these conditions was treated as incompressible ($\alpha = 0$). At $v_0 t/x_0 = 1.1$, the relative viscosity at the centreline attains its *maximum* value of approximately 300, causing it to behave much like an elastic solid. The fluid

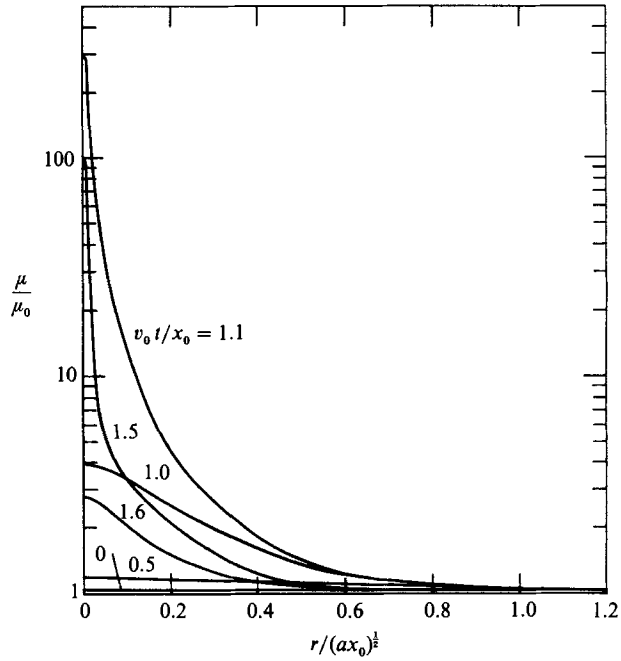

FIGURE 5. The relative viscosity profile at various instances in time for a collision between rigid spheres in an incompressible fluid with $St = 3.5$ and $\eta = 10^{-3}(St_3^* = 3.5)$.

near $r = 0$ is extremely resistant to flow and strongly resists the close approach of the spheres. For $St > St_3^*$, this dramatic increase in viscosity concentrated near the centreline is even greater and causes difficulties in the numerical solution.

4.2. *Results for elastic spheres*

There is a remarkable difference in the characteristics of the rebound following the collision between elastic spheres and those associated with the rebound of rigid spheres caused solely by fluid compression. This difference is illustrated in figure 6, which shows the total dimensionless force between colliding spheres as a function of time for $\alpha = 10^{-2}$, $\eta = 0$, $St = 5$, and various ϵ. For $\epsilon \leqslant 10^{-6}(St_1^* \gg St_2^* = 2.3$, $x_1 \ll x_2)$, the elasticity of the spheres is too small to affect the rebound process. This weak rebound is due to fluid compression and expansion, as discussed in §4.1. When $v_0 t/x_0 \geqslant 2.2$, the spheres have essentially come to rest, although damped oscillations occur which have a negligible effect on the final position. For $\epsilon \geqslant 10^{-4}(St_1^* < St = 5)$, the energy stored in elasticity dominates that stored in compressibility, and a more significant rebound results. For $\epsilon = 10^{-4}(St_1^* = 3.7)$, the maximum force during approach is only 70% of that for inelastic collisions, but the maximum suction force during rebound increases by a factor of almost 5. For more elastic collisions, the influence of fluid compression, and the corresponding energy stored in the compressed fluid, is relatively small. The maximum force continues to decrease, and the maximum suction force during rebound also decreases since the minimum distance of approach increases and the fluid can more easily enter this larger gap. We caution, however, that the suction (negative) forces shown in figure 6 may not be realized in practice because of cavitation.

The remarkable difference in collisions of elastic spheres compared to those of rigid spheres is also exemplified in figure 7, a diagram of the minimum separation of

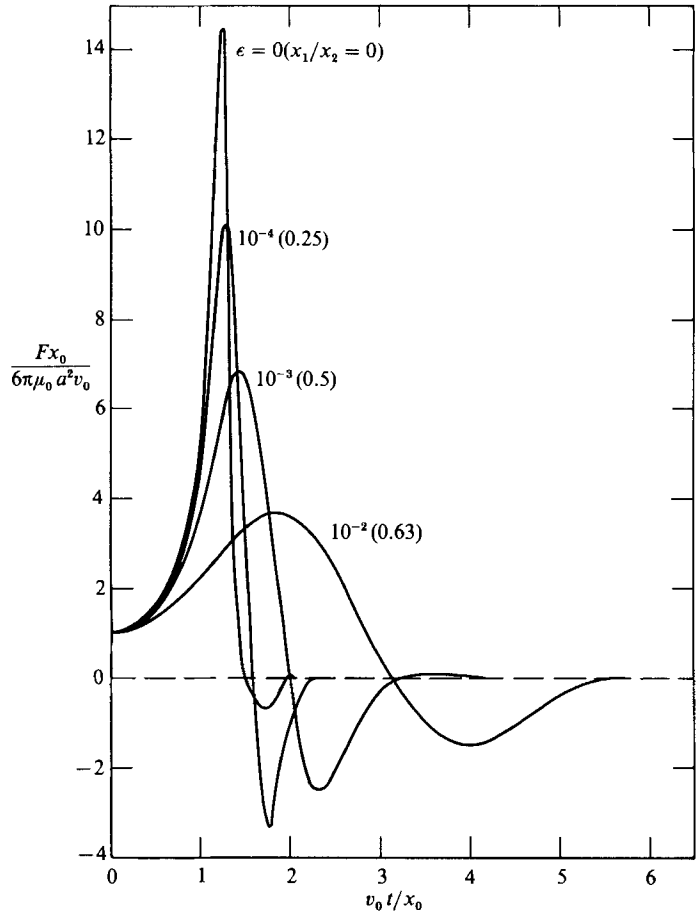

FIGURE 6. The dimensionless hydrodynamic force as a function of dimensionless time for $St = 5$, $\alpha = 10^{-2}$, $\eta = 0$ and several values of the elasticity parameter, ϵ.

approach and maximum rebound separation at the centreline as a function of St. The straight, solid line corresponds to both the minimum and maximum separation of rigid spheres in incompressible fluids. The pair of dotted lines form an envelope and correspond to the minimum (lower line) and maximum (upper line) centreline separations which occur during the approach and rebound, respectively, of rigid spheres ($\epsilon = 0$) in a compressible fluid with $\alpha = 10^{-2}(St_2^* = 2.3)$. During collisions for which $St \leqslant 4.5$, the spheres bounce slightly owing to fluid compression and decompression before they reach $x/x_0 = \exp(-St)$. For $St > 4.5$, the minimum separation drops below that of the incompressible case, since the fluid can both compress as well as squeeze out of the gap, causing the maximum pressure to increase dramatically. The maximum rebound separation increases relative to the corresponding minimum separation but its absolute value decreases with increasing St. In contrast, the pair of dashed lines correspond to the minimum and maximum separations which occur during the collision between elastic spheres in an incompressible fluid ($\alpha = 0$) with $\epsilon = 10^{-2}(St_1^* = 1.8)$. For these elastic collisions, the minimum separation is much larger and is relatively independent of St for $St \gg St_1^*$. The maximum rebound separation decreases with increasing St for small values of St owing to the increased inertia bringing the spheres closer together, but it

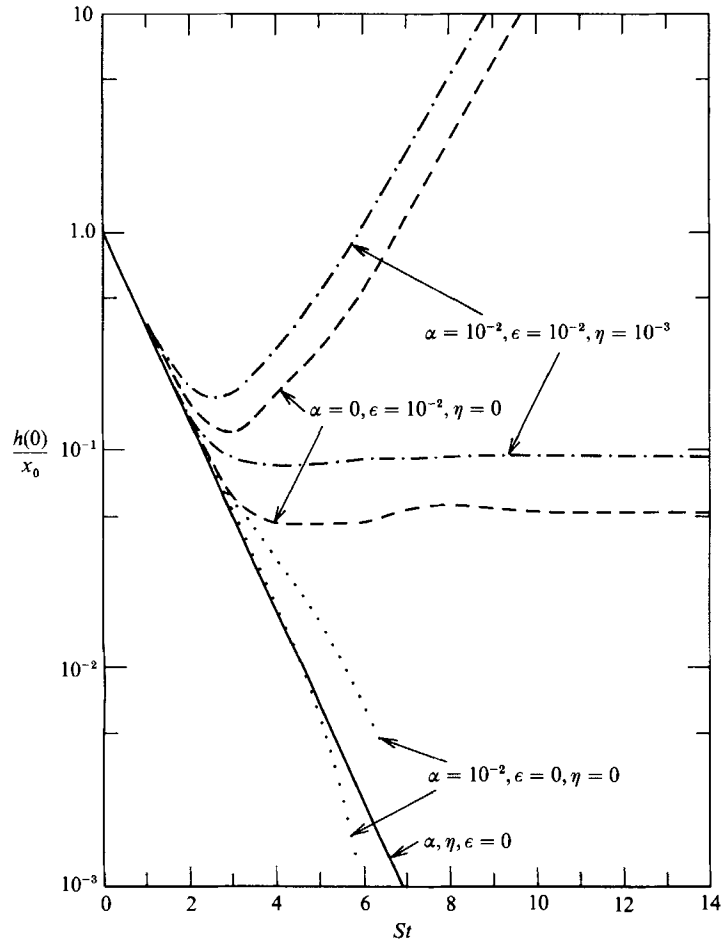

FIGURE 7. The minimum centreline separation prior to rebound and maximum centreline separation subsequent to rebound as functions of the inertia parameter, St.

increases steadily for $St \geqslant 3.0$ owing to the increased deformation and rebound for the more energetic collisions. For $St > 7$, this maximum rebound separation is larger than the original dimensionless separation of unity. This separation will be even larger when cavitation occurs. Finally, the dashed-dotted lines, corresponding to the minimum and maximum separations when the effects of fluid compression, viscosity changes, and solid elastic deformation are all included, show that fluid property changes have a rebound-enhancing effect, but that the qualitative features of the collision dynamics are similar to those when the fluid properties are constant and only solid deformation is included.

Figure 8, a plot of the dimensionless maximum rebound velocity, v_{mr}/v_0, as a function of St, further illustrates the rebound enhancement due to fluid compression and viscous increases. For comparison, the solid lines represent the maximum rebound velocities which occur during incompressible, isoviscous elastic collisions for various ϵ. As St increases, the spheres naturally rebound with a greater velocity because their increased inertia leads to higher pressures and hence more energy stored in elastic deformation prior to rebound. During the early stages of rebound, the centres of masses of the two spheres are moving apart, but the deformed surfaces

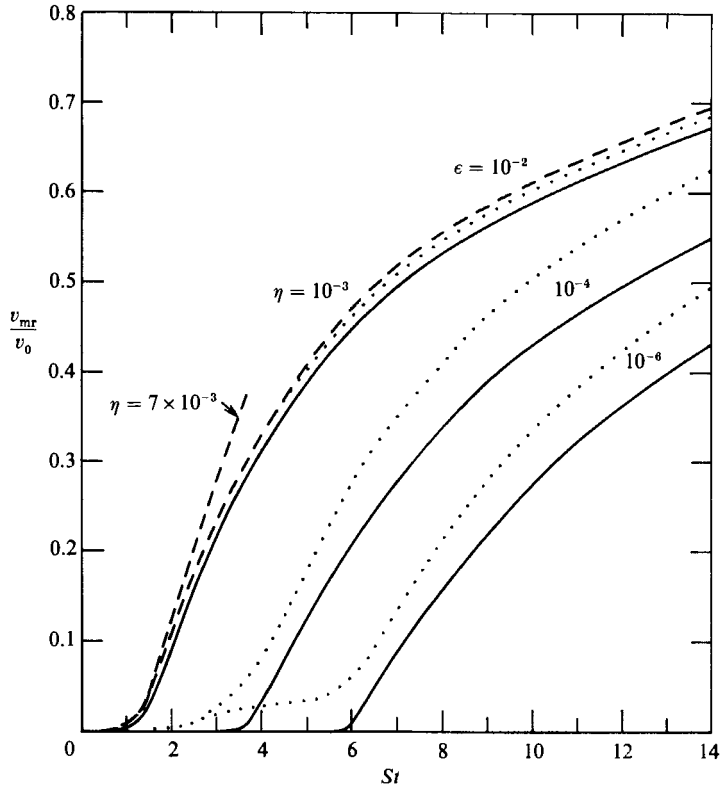

FIGURE 8. The maximum relative rebound velocity of elastic spheres as a function of the inertia parameter, St. The solid lines are for constant fluid properties ($\alpha = \eta = 0$), the dotted lines are for compressible, isoviscous fluids ($\alpha = 10^{-2}$, $\eta = 0$) and the dashed lines are for variable fluid density and viscosity ($\alpha = 10^{-2}$, $\eta = 10^{-3}$, 7×10^{-3}).

are still moving toward one another as the stored elastic energy is released and converted into kinetic energy and viscous work. The maximum rebound velocity occurs at the time when the lubrication force drops to zero. As mentioned previously, any cavitation would occur after this time and so would not affect the maximum rebound velocity. When the influence of fluid compression ($\alpha = 10^{-2}$) is included in the model, as shown by the dotted lines, the rebound velocity is increased. When $\epsilon = 10^{-2}(St_1^* = 1.8)$ and $\alpha = 10^{-2}(St_2^* = 2.3)$, only a slight enhancement of the rebound velocity is predicted for all values of St. However, for $\epsilon = 10^{-4}(St_1^* = 3.7)$, and the same value of $\alpha = 10^{-2}(St_2^* = 2.3)$, the maximum rebound velocity is increased by about 20% over that for an incompressible fluid at $St = 10$. Moreover, at low St (e.g. $St = 3$), for which $St > St_2^*$ but $St < St_1^*$, a weak but measurable rebound resulting primarily from fluid compression is predicted, whereas no rebound is predicted to occur had the fluid been treated as incompressible. This effect is even more dramatic for $\epsilon = 10^{-6}$ and $\eta = 10^{-2}$.

Although there is a small enhancement of rebound due to fluid compression between elastic spheres, there is a much greater effect on the collision between elastic spheres as a result of the increase in viscosity with pressure. Two exemplary cases of the influence of fluid viscosity are shown in figure 8. One dashed line corresponds to $\epsilon = 10^{-2}$, $\alpha = 10^{-2}$ and $\eta = 10^{-3}(St_3^* = 3.5)$ and shows that there is only a small enhancement of rebound when viscosity effects are small and $St_1^* \ll St_3^*$. The other

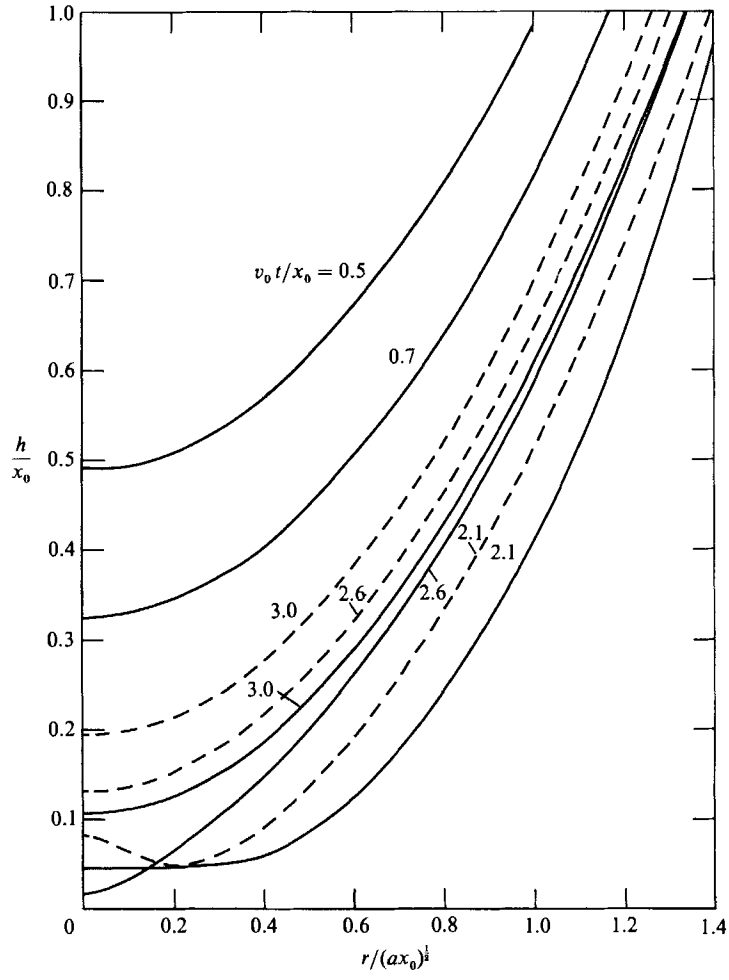

FIGURE 9. The deformed gap profile at several instances in time for an elastic collision with $St = 6$, $\epsilon = 10^{-3}$, $\alpha = 0$, and $\eta = 0$ (solid lines) and $\eta = 6 \times 10^{-4}$ (dashed lines).

dashed line in figure 8, corresponding to $\eta = 7 \times 10^{-3}(St_3^* = 2.5)$ and the same values of α and ϵ, clearly shows that as $St \to St_3^*$, a significant enhancement of the rebound velocity occurs. This enhancement is primarily due to the sharp increase in viscosity near the centreline of the two spheres, which serves to strongly resist their relative motion and to cause additional elastic deformation.

Figure 9 shows this increased-viscosity effect more clearly. This figure gives the dimensionless gap profile as a function of radial distance at several times for the specific case of $St = 6$ and $\epsilon = 10^{-3}(St_1^* = 3.5)$. The solid lines in this figure correspond to incompressible, isoviscous, elastic collisions; whereas the dashed lines show the influence of pressure-dependent viscosity with $\eta = 6 \times 10^{-4}(St_3^* = 3.7)$. For short times ($v_0 t/x_0 \leqslant 0.7$), the profiles are identical. At later times (e.g. $v_0 t/x_0 = 2.1$), the isoviscous case reveals that the noses of the two spheres have flattened owing to the high pressure in the fluid between the approaching surfaces. This centreline deformation is increased dramatically when the fluid viscosity is allowed to increase with pressure, and a pronounced dimple forms around the axis of symmetry. The marked increase of viscosity with pressure results in a fluid which behaves much like

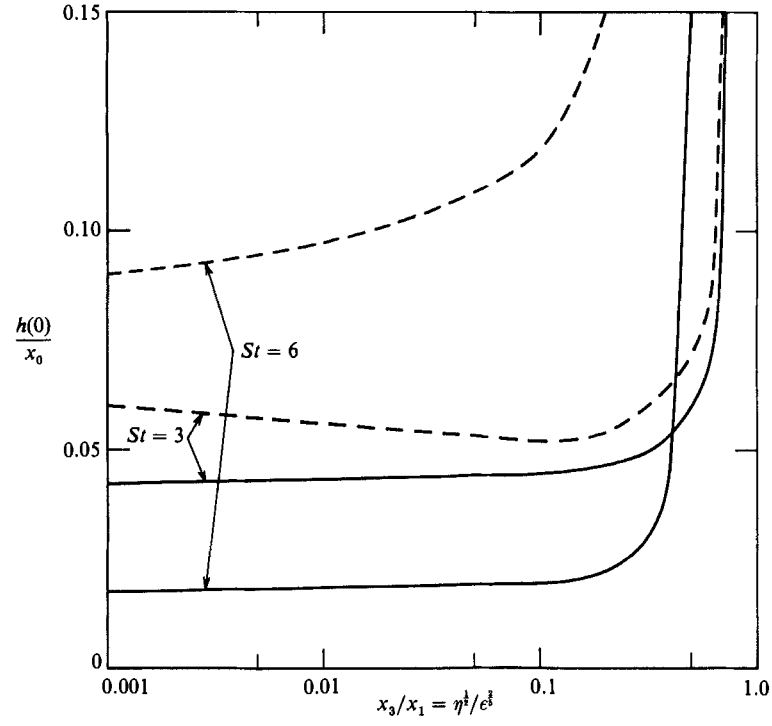

FIGURE 10. The minimum distance of approach (solid lines) and maximum rebound separation (dashed lines) at the centreline as functions of the ratio of the viscosity and deformation lengthscales, x_3/x_1, for $St = 3$ and 6.

a solid – very resistant to flow – and prevents the nose of the sphere from approaching further. The fluid near the centre is nearly trapped in this dimple; the sphere bounces from a larger minimum centreline separation, and a larger maximum rebound separation is reached. This dimple formation and increase in minimum separation were also predicted by Lee & Cheng (1973) in the investigation of two lubricated cylinders.

Finally it is informative to look at the relative influences of the effects of fluid viscosity changes and solid elasticity. Figure 10 shows a plot of the minimum distances of approach and maximum rebound separations which occur at the centreline for $St = 3$ and 6 as functions of the ratio of the viscous and elastic lengthscales: x_3/x_1. For $x_3 \ll x_1$, the spheres do not become close enough for significant viscosity changes to occur, and elasticity effects dominate the collision process. However, as $x_3/x_1 \to 1$, The influence of viscosity changes on the collision becomes dramatic, resulting in increased minimum and maximum separations. This increase is extremely abrupt and results from the increased resistance to flow of the fluid. As discussed previously, the maximum separations subsequent to rebound will be even greater when cavitation occurs.

4.3. *Concluding remarks*

It has been shown that the large hydrodynamic pressures required to deform the surfaces of two elastic spheres as they collide also dramatically increase the density and viscosity of the fluid in the gap. Whereas the magnitude of the elastic deformation of the surfaces was previously thought to be the primary factor in

determining whether or not the spheres rebound, the changes which occur to the fluid density and viscosity may also play important roles. In particular, changes in the fluid density alone can cause rebound of even perfectly rigid spheres, although this rebound is relatively weak. The viscosity of the fluid in the gap between the colliding spheres may increase by several orders of magnitude very near the centreline, causing the fluid to behave much like an elastic solid and producing a pronounced dimple of the elastic surface.

Under typical conditions, such as those present during inertial filtration of aerosols where either the particles or surfaces have been covered with a viscous liquid, the gap lengthscales at which solid deformation, fluid compression and viscosity become important are approximately equivalent. Therefore, each of these effects plays an important role in influencing the collision and rebound process. Under these conditions, the changes in fluid density and viscosity with pressure lead to moderate quantitative changes in the collision parameters such as the minimum distance of approach, the value of St required for rebound, and the maximum rebound velocity achieved. However, the qualitative features of the collision and rebound process are generally the same as those predicted with constant fluid properties. In contrast, collisions involving absolutely rigid spheres have drastically different characteristics to those involving slightly elastic spheres.

This work was undertaken with support of the National Science Foundation under grants CBT-8414743 and CBT-8451014.

REFERENCES

ASME 1953 Viscosity and density of over 40 fluids at pressures to 15,000 p.s.i. and temperatures at 425 °F. Research Committee on Lubrication. ASME.

Barnocky, G. 1988 Collisions between elastic particles or spherical drops in viscous fluids. Ph.D. Thesis, University of Colorado.

Barnocky, G. & Davis, R. H. 1988*a* The effect of Maxwell slip on the aerodynamic collision and rebound of spherical particles. *J. Colloid Interface Sci.* **121**, 1.

Barnocky, G. & Davis, R. H. 1988*b* Elastohydrodynamic collision and rebound of spheres: experimental verification. *Phys. Fluids* **31**, 1324.

Butler, H. 1960 The hydrodynamic effect between approaching surfaces with interposed viscous fluid films and its influence on surface deformations. *J. Inst. Petrol.* **46**, 435.

Christensen, H. 1962 The oil film in a closing gap. *Proc. R. Soc. Lond.* A **226**, 312.

Christensen, H. 1970 Elastohydrodynamic theory of spherical bodies in normal approach. *Trans. ASME* F: *J. Lubric. Tech.* **92**, 1.

Chu, P. S. Y. & Camerson, A. 1962 Pressure viscosity characteristics of lubricating oils. *J. Inst. Petrol.* **48**, 147.

Dahneke, B. 1971 The capture of aerosol particles by surfaces. *J. Colloid Interface Sci.* **37**, 342.

Davis, R. H., Serayssol, J.-M. & Hinch, E. J. 1986 The elastohydrodynamic collision of two spheres. *J. Fluid Mech.* **163**, 479.

Dowson, D. & Higginson, G. R. 1977 *Elastohydrodynamic Lubrication.* Pergamon.

Dowson, D. & Taylor, C. M. 1979 Cavitation in bearings. *Ann. Rev. Fluid Mech.* **11**, 35.

Finkin, E. F. 1973 Experimental investigation of spherical impact, both dry and with a fluid film. *Trans. ASME* F: *J. Lubric. Tech.* 95.

Gal, E., Tardos, G. & Pfeffer, R. 1985 A study of inertial effects in granular bed filtration. *J. Fluid Mech.* **31**, 1093.

Grubin, A. N. & Vinogradova, I. E. 1949 Central Scientific Research Institute for Technology and Mechanical Engineering, Book 30, Moscow. (DSIR Translation No. 337).

HERREBRUGH, K. 1970 Elastohydrodynamic squeeze films between two cylinders in normal approach. *Trans. ASME*: *J. Lubric. Tech.* **92**, 292.

HERSEY, M. D. & HOPKINS, R. F. 1954 Viscosity of lubricants under pressure, report to ASME Research Committee on Lubrication.

HOCKING, L. M. 1973 The effect of slip on the motion of a sphere close to a wall and of two adjacent spheres. *J. Engng Maths* **7**, 207.

LEE, K. M. & CHENG, H. S. 1973 The pressure and deformation profiles between two normally approaching lubricated cylinders. *Trans. ASME* F: *J. Lubric. Tech.* **95**, 308.

LOFFLER, F. 1980 Problems and recent advances in aerosol filtration. *Separ. Sci. Technol.* **15**, 297.

LOVE, A. E. H. 1927 *A Treatise on the Mathematical Theory of Elasticity*, 4th edn. Dover.

SERAYSSOL, J.-M. & DAVIS, R. H. 1986 The influence of surface interactions on the elastohydrodynamic collision of two spheres. *J. Colloid Interface Sci.* **114**, 1.

TABOR, D. 1949 Collisions through fluid layers. *Engineering* **2**, 145.

WEAST, R. C. (ED.) 1974 *Handbook of Chemistry and Physics*. CRC Press.